International Journal of Thermophysics, Vol. 19, No. 4, 1998

Density Relaxation of Liquid–Vapor Critical Fluids in Earth's Gravity[1]

R. A. Wilkinson[2]

Experimental results of the density relaxation of a liquid–vapor critical fluid in Earth's gravity over a temperature regime of severe density stratification are presented. A 10-mm-diameter × 1-mm-thick disk-shaped sample of SF_6 was placed in a Twyman–Green phase shifting interferometer with a phase uncertainty of 1/65 of a wavelength over 60 h. Relaxations to equilibrium stratification were observed for a temperature range from 1.0 to 29.6 mK above T_c, where T_c is the critical temperature. The interferometry provided a density distribution history over the full extent of the sample cell. Two types of initial density states were established before stepping to the final temperature (density) states for relaxation: (1) the two-phase state at $T_c - 50$ mK and (2) the equilibrium state at $T_c + 100$ mK. Upper and lower portions of the cell relaxed differently for these two initial states. For the $T_c + 100$ mK initial state, relaxation to $T < T_c + 3$ mK showed an early density overshoot followed by an additional long-time relaxation not seen in the other relaxation sequences. Otherwise, relaxations were faster and increasingly nondiffusive (without a unique exponential description) as the final state became closer to the critical temperature.

KEY WORDS: critical point; density; liquid–vapor critical point; sulfur hexafluoride.

1. INTRODUCTION

Earth-based room-temperature liquid–vapor critical fluid experiments are infrequently performed closer than 30 mK above the critical temperature, T_c, because of the effects of gravitational stratification on the interpretation of results [1]. However, there are some early theory and experiments that considered thermal relaxation times and mechanisms in this regime [2–5].

[1] Paper presented at the Thirteenth Symposium on Thermophysical Properties, June 22–27, 1997, Boulder, Colorado, U.S.A.

[2] Microgravity Fluid Physics Branch, NASA Lewis Research Center, Cleveland, Ohio 44135, U.S.A.

0195-928X/98/0700-1175$15.00/0

Since the 1980s there have been a number of microgravity experiments that examined equilibration and have been performed with $\varepsilon < 10^{-4}$, $\varepsilon \equiv (T - T_c)/T_c$ [6–9]. Those experiments resolved some early confusion about how fast a critical fluid equilibrates in low gravity. To complement the low gravity experiments, this paper presents similar experiments in Earth's gravity.

In recent years several groups have worked on experiments and models [10–13] to describe density relaxation of one-phase systems in Earth's gravity. Those models have examined various combinations of: one or two dimensions, small or slow temperature changes relatively far from T_c, variable and fixed thermophysical properties, and approximate equations of state to enable tractable computations. Other groups have worked on the equilibration of critical binary mixtures as they transition from a two-phase state to a one-phase state by tracking the surface tension evolution [14, 15]. The complete understanding of liquid–vapor critical fluid equilibration in 1g is more difficult than in low g, because divergent thermophysical properties and compressible fluid hydrodynamics mix in complicated ways.

The observation technique of choice in this work was interferometric imaging. This technique allowed resolution in two dimensions with no thermal or geometrical perturbation to the sample.

This paper presents experimental observations with two kinds of initial conditions and relatively large temperature changes to the final state. Section 2 presents some of the experimental configurations and procedures. Section 3 presents results, and Section 4 offers conclusions.

2. EXPERIMENTAL PROCEDURE

This work collected Earth-based interferometric data from a 10-mm-diameter × 1-mm-thick disk volume of sulfur hexafluoride (an equivalent sample to that used for low-g experiments [9]). The gravitational vector was along a diameter of the disk. We found that if the g-vector was along the cylindrical axis (optical axis) of the disk, then the interferometric signal had vanished by the time the thermostat had achieved any new set points. Hence, we could not examine this orientation, which would have been the best comparison to what we observed in low gravity.

The interferometer was a compact Twyman–Green configuration contained inside a thermostat with better than $\pm 50\,\mu$K control. The cell was loaded to $\rho_c - 0.05\%$ $(+0.20 - 0.00\%)$, where ρ_c is the critical density. The density precision was determined by statistically sampling the meniscus location just below T_c. The average position was calibrated using equilibrium calculations of the meniscus position for various misfilled samples with

identical geometry and fill tube orientation as our cell. The critical temperature was 45.4630 ± 0.0003°C as measured with a YSI Type 44014 thermistor thermal epoxied into a cell flange about 1 cm from the nearest fluid boundary. The uncertainty in T_c was caused primary by ambiguity of the appearance of the phase transition in a stratified sample viewed interferometrically.

The thermostat consisted in part of two PID-controlled temperature shells of aluminum. A third, the innermost, shell was an 11-cm-long × 6-cm-diameter aluminum sample cell holder. The sample cell holder contained the fluid cell and the Twyman–Green interferometer. The compact interferometer under tight temperature control greatly enhanced optical phase resolution. The short-term phase resolution in this work was better than 1/470 of a wavelength, λ, while the long-term phase resolution was $\lambda/65$ over 60 h. The cell, shown schematically in Fig. 1, was designed for minimal thermal gradients and low thermal masses. Temperature changes from the initial to the final temperature state required 15 to 19 min, with no overshoot. The optical layout details are best described in a complementary paper on phase shifting interferometry [16].

Experimental operations were automated for both temperature control and image capture with runs up to 50 h in duration. A sequence of 16 image captures was executed in less than 6 s to constitute one snapshot of the fluid density. The number of images and the timing were convenient choices based on image memory limits of the frame-grabber board and the

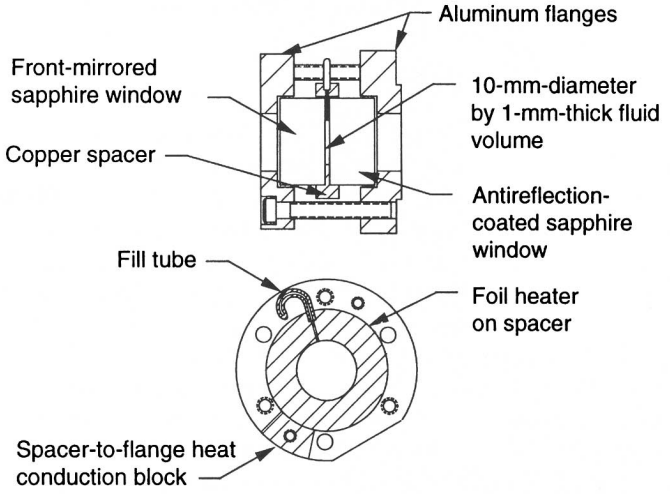

Fig. 1. Fluid cell for interferometric measurements. The foil heater was not used in this work.

settling time of the liquid–crystal phase shifter. The frame-grabber was set up to utilize the middle 80% of the 8-bit intensity dynamic range. A data set consisted of four final states (nominally 30, 10, 3, and 1 mK above T_c) from each of two initial states (100 mK above T_c and 50 mK below T_c). Hence, there were eight runs in a data set. A run would last more than five time constants as predicted from a diffusive model and low-gravity experiments. There were at least 100 capture sequences of 16 images each during a run.

The phase shifting Twyman–Green interferometer was designed to use the Carré technique of analysis. The technique required four images distinguished by a fixed relative phase shift to calculate one optical phase map. A 16-image sequence, thereby, gave four sets of four images (four phase maps) to allow some data averaging. The Carré technique produced a two-dimensional pixelwise array of phase values for each snapshot in time. The arrays were 540 pixels high × 480 pixels wide in each image and phase map. The last phase map acquired in a run was used as a reference map and subtracted from all the other maps. Using such a reference phase map eliminated fixed phase shifts from the optics and referenced the data with respect to a nominal fluid equilibrium. Pixels beyond the fluid boundary were masked out in the final analysis.

The 540 horizontal pixel rows were divided into strips, 3 pixels high, and assigned a height with respect to the horizontal layer where the

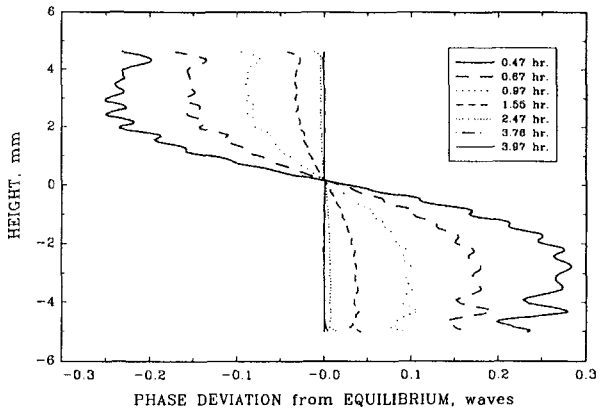

Fig. 2. Height profiles of deviation from equilibrium with time for a run with an initial state of $T_c - 50$ mK and a final state of $T_c + 29.6$ mK. The earliest and latest times plotted reflect the time window when the thermostat was stable to $\pm 50\,\mu$K. One wave (fringe) of phase deviation corresponds to a 0.35% density deviation.

meniscus forms. There were 168 such strips that spanned the 1-cm fluid diameter. All the pixels in each of the strips were averaged to determine a phase shift per height. Each average included 700 to 1400 pixels. A data set then provides a measure of fluid density *deviation from equilibrium* as a function of height and time (Fig. 2).

The final step of analysis was the fitting of a time sequence of deviations at a given height to an exponential function that was used for the low-gravity experiments [9]. The phase at height h, ϕ_h, was fit to

$$\phi_h(t) = K + A\{e^{(-t/\tau)} - e^{(-t_r/\tau)}\} \tag{1}$$

where t is time, t_r is the time of the reference phase map that is subtracted, and K, A, and τ are fitting parameters.

3. RESULTS

The results in Figs. 2 and 3 show extreme examples of the fluid's height versus density deviation time evolution. To facilitate understanding of the results, it should be noted that there was a 0.35% density deviation per fringe (wave) of phase shift for this 1-mm-thick fluid sample. Both figures show a different time evolution between the upper and the lower cell halves, and a conspicuous density overshoot in each half of the cell is shown in Fig. 3. There is a visible ripple in the traces of both figures that

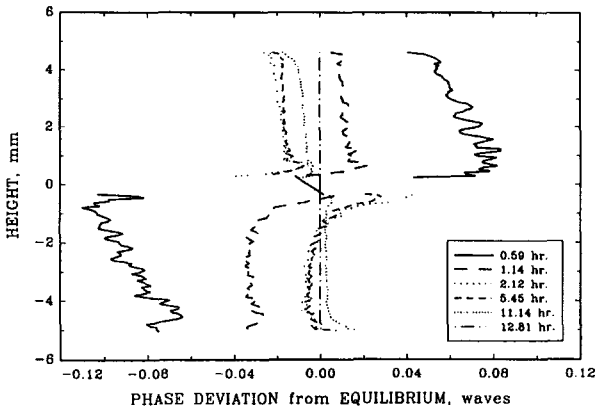

Fig. 3. Height profiles for a run with an initial state of $T_c + 100$ mK and a final state of $T_c + 2.8$ mK. Note the geometric time sequence of the plots. Ignore the traces in the height region ± 0.5 mm about 0 because the fringes were too closely packed for reliable analysis.

diminishes with time. The ripple evident in the one-phase to one-phase relaxation contains more and higher spatial frequencies than in the two-phase to one-phase relaxation. This ripple is evident even when the thermometry is stable to the specification of $\pm 50\,\mu$K. The initial temperature change transients of a run provided a severe perturbation of the fluid this close to the critical point. The interpretation of the ripple observation is that the fluid boundary layers on the sapphire windows are not of uniform thickness and changing with time. Surface flows of different character might be expected in these two runs.

Next the time dependence at selected heights is examined. Figure 4 represents the best fit to Eq. (1). For this run the time constant was significantly longer at all heights in the sample than it was for a low-g experiment. The run begins to overlap with the temperature regime explored by May and Maher [14]. Even though May worked with incompressible binary mixtures, the findings of a slower late-stage relaxation of the interface than a diffusion model predicts parallel our observation. Figure 5 represents a run where the initial state, $T_c + 100$ mK, was different from that in Fig. 4. The height position was selected closer to the meniscus to emphasize the initial asymmetry of the relaxation in the vapor-like and liquid-like portions of the cell. In low gravity, relaxation results were not sensitive to whether the initial state was either two-phase or one-phase [9]. Figure 6 represents further anomalies for a one-phase to one-phase

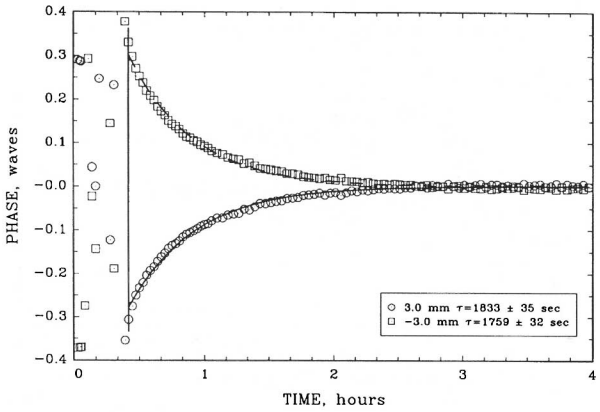

Fig. 4. Relaxation at 3 mm above and below the meniscus for a run with an initial state at $T_c - 50$ mK and a final state of $T_c + 29.6$ mK. In low gravity the longest time constant was 1087 ± 10 s at $T_c + 28.7$ mK. The vertical line indicates the beginning of the fit to Eq. (1). The key notes the fit exponential time constants and their fit uncertainties.

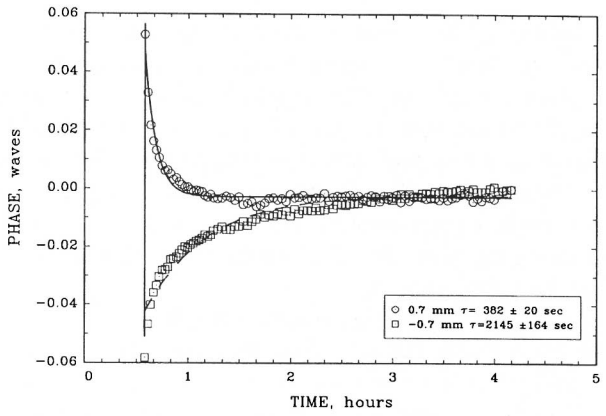

Fig. 5. Relaxation at 0.7 mm above and below the meniscus for a run with an initial state at $T_c + 100$ mK and a final state of $T_c + 29.6$ mK. The key notes the fit exponential time constants and their fit uncertainties.

experimental run. With the final state at $T_c + 2.8$ mK, two quite different relaxation time scales are observed. It appears that the longest time scale is not completely captured even in the more than eight time constants predicted from low-gravity work. An overshoot of the density occurs in both the liquid-like and the vapor-like portions of the fluid, still with an asymmetry.

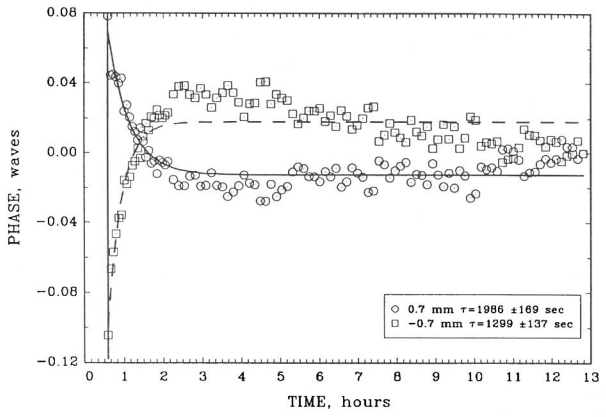

Fig. 6. Relaxation at 0.7 mm above and below the meniscus for a run with an initial state at $T_c + 100$ mK and a final state of $T_c + 2.8$ mK. In low gravity the time constant was 5546 ± 62 s at $T_c + 3.4$ mK. The key notes the fit exponential time constants and their fit uncertainties.

4. CONCLUSIONS

Experimental results of the full-field density relaxation of a liquid–vapor critical fluid in Earth's gravity over a temperature regime of severe density stratification were presented. Relaxations to equilibrium stratification were observed for a temperature range from 1.0 to 29.6 mK above T_c, where T_c is the critical temperature. Two types of initial density states were established before stepping to the final temperature (density) states for relaxation: (a) the two-phase state at $T_c - 50$ mK and (b) the equilibrium state at $T_c + 100$ mK. Upper and lower portions of the cell relaxed differently for these two initial states. Different heights within each cell half relaxed with different nominal time constants. For the $T_c + 100$ mK initial state, relaxation to $T < T_c + 3$ mK showed an early density overshoot followed by an additional long-time relaxation not seen in the other relaxation sequences. Two-phase to one-phase relaxations were faster than diffusion close to T_c. However, for $T \geqslant T_c + 30$ mK, these relaxations become slower than diffusive. In general, final relaxations were increasingly nondiffusive (without a unique exponential description) as the final state became closer to the critical temperature.

ACKNOWLEDGMENTS

This work was performed at NASA Lewis Research Center in Cleveland, Ohio, as part of the Microgravity Fluid Physics Branch. The author would like to thank Christoph Bartscher, Mike Bayda, and Gary Fiedler for substantial help in setting up the experiment. Also, the understanding of this work has benefited greatly from discussions with Hacene Boukari, Robert Berg, Robert Gammon, Greg Zimmerli, Kyung-Yang Min, James Maher, and Horst Meyer.

REFERENCES

1. M. R. Moldover, J. V. Sengers, R. W. Gammon, and R. J. Hocken, *Rev. Mod. Phys.* **51**:79 (1979).
2. M. Sh. Giterman and V. A. Shteinberg, *Teplofiz. Vyslokikh Temp.* **10**:565 (1972) [*High Temp.* **10**:501 (1972)].
3. D. Dahl and M. R. Moldover, *Phys. Rev. A* **6**:1915 (1972).
4. M. Gitterman, *Rev. Mod. Phys.* **50**:85, Part I (1978).
5. T. J. Edwards, *Specific Heat Measurements Near the Critical Point of Carbon Dioxide*, Ph.D. thesis (Department of Physics, University of Western Australia, 1984).
6. J. Straub and K. Nitsche, *Fluid Phase Equil.* **88**:183 (1993).
7. J. Straub, L. Eicher, and A. Haupt, *Phys. Rev. E* **51**:5556 (1995).
8. T. Fröhlich, P. Guenoun, M. Bonetti, F. Perrot, D. Beysens, Y. Garrabos, B. LeNeindre, and P. Bravais, *Phys. Rev. E* **54**:1544 (1996).

9. R. A. Wilkinson, G. A. Zimmerli, H. Hao, M. R. Moldover, R. F. Berg, W. L. Johnson, R. A. Ferrell, and R. W. Gammon, *Phys. Rev. E* **57**:436 (1998).
10. R. F. Berg, *Phys. Rev. E* **48**:1799 (1993).
11. H. Boukari, R. L. Pego, and R. W. Gammon, *Phys. Rev. E* **52**:1614 (1995).
12. F. Zhong and H. Meyer, *Phys. Rev. E* **51**:322 (1995).
13. B. Zappoli, S. Amiroudine, P. Carles, and J. Ouazzani, *J. Fluid Mech.* **316**:53 (1996).
14. S. E. May and J. V. Maher, *Phys. Rev. Lett.* **67**:2013 (1991).
15. W.-J. Ma, P. Keblinski, A. Maritan, J. Koplik, and J. R. Banavar, *Phys. Rev. Lett.* **71**:3465 (1993).
16. M. R. Bayda, C. Bartscher, R. A. Wilkinson, and G. A. Zimmerli, Paper presented at the 13th Symp. Thermophys. Prop., Boulder, CO (1997).